Molecules and Cells

Therapeutic Benefits of Mesenchymal Stromal Cells in a Rat Model of Hemoglobin-Induced Hypertensive Intracerebral Hemorrhage

Rui Ding[1,4], Chunnan Lin[2,4,*], ShanShan Wei[3], Naichong Zhang[2], Liangang Tang[2], Yumao Lin[2], Zhijun Chen[1,*], Teng Xie[1], XiaoWei Chen[1], Yu Feng[1], and LiHua Wu[1]

[1]Department of Neurosurgery, Jingmen No. 1 People's Hospital, Jingmen 448000, Hubei, China, [2]Department of Neurosurgery, Maoming People's Hospital, Maoming 525000, Guangdong, China, [3]Department of Hematology, Jingmen No. 1 People's Hospital, Jingmen 448000, Hubei, China, [4]These authors contributed equally to this work.
*Correspondence: 470681525@qq.com (CL); 415038939@qq.com (ZC)
http://dx.doi.org/10.14348/molcells.2017.2251
www.molcells.org

Previous studies have shown that bone marrow mesenchymal stromal cell (MSC) transplantation significantly improves the recovery of neurological function in a rat model of intracerebral hemorrhage. Potential repair mechanisms involve anti-inflammation, anti-apoptosis and angiogenesis. However, few studies have focused on the effects of MSCs on inducible nitric oxide synthase (iNOS) expression and subsequent peroxynitrite formation after hypertensive intracerebral hemorrhage (HICH). In this study, MSCs were transplanted intracerebrally into rats 6 hours after HICH. The modified neurological severity score and the modified limb placing test were used to measure behavioral outcomes. Blood-brain barrier disruption and neuronal loss were measured by zonula occludens-1 (ZO-1) and neuronal nucleus (NeuN) expression, respectively. Concomitant edema formation was evaluated by H&E staining and brain water content. The effect of MSCs treatment on neuroinflammation was analyzed by immunohistochemical analysis or polymerase chain reaction of CD68, Iba1, iNOS expression and subsequent peroxynitrite formation, and by an enzyme-linked immunosorbent assay of pro-inflammatory factors (IL-1β and TNF-α). The MSCs-treated HICH group showed better performance on behavioral scores and lower brain water content compared to controls. Moreover, the MSC injection increased NeuN and ZO-1 expression measured by immunochemistry/immunofluorescence. Furthermore, MSCs reduced not only levels of CD68, Iba1 and pro-inflammatory factors, but it also inhibited iNOS expression and peroxynitrite formation in perihematomal regions. The results suggest that intracerebral administration of MSCs accelerates neurological function recovery in HICH rats. This may result from the ability of MSCs to suppress inflammation, at least in part, by inhibiting iNOS expression and subsequent peroxynitrite formation.

Keywords: hypertensive intracerebral hemorrhage, iNOS, mesenchymal stromal cells, $ONOO^-$

INTRODUCTION

The Intracerebral hemorrhage (ICH) is a subtype of stroke, characterized by high morbidity, high mortality, and poor clinical outcome (Balami and Buchan, 2012; Qureshi et al., 2009). Despite the great improvements in patient outcome following supportive care or surgical evacuation of the hematoma (Candelise et al., 2007), there are no specific, validated treatments available so far for ICH. The inflammatory response is regarded as an important contributor to ICH-induced brain injury (Aronowski and Hall, 2005). ICH induces an acute inflammatory response accompanied by leucocytes infiltration and activation of microglia (Gong et al.,

Received 25 October, 2016; revised 29 December, 2016; accepted 9 January, 2017; published online 13 February, 2017

eISSN: 0219-1032

2000). Anti-inflammatory strategies have been proven to be especially effective in the treatment of ICH (Jung et al., 2004; Masada et al., 2001).

Mesenchymal stromal cells (MSCs) have both immunosuppressive properties and the capacity for multi-differentia- tion (Vaquero et al., 2013; Yan et al., 2013). They not only interact with immune cells, but also inhibit their functions (Di Nicola et al., 2002; Meirelles et al., 2009; Yan et al., 2013). For example, Yan et al found that MSCs had the ability to maintain the resting phenotype of microglia or to control microglial activation by inhibiting the proliferation and phagocytic capacity of microglia and inducing apoptosis in microglia (Yan et al., 2013). Furthermore, the beneficial effects of MSCs have been reported in animal exprimental models of ICH, in which they suppress the inflammatory response, reduce brain edema and tissue damage, and improve angiogenesis and functional deficits (Fatar et al., 2008; Liang et al., 2013; Liao et al., 2009; Seyfried et al., 2010; Wang et al., 2012). Beneficial effects have also been noted in stroke-related clinical trials (Steinberg et al., 2016). However, the underlying molecular mechanisms for the effects of MSCs are still unknown.

Peroxynitrite ($ONOO^-$) is a strong oxidizing and nitrating agent (Beckman and Koppenol, 1996; Pacher et al., 2007), which is mainly generated by inducible nitric oxide synthase (iNOS) (Hirabayashi et al., 2000). Research findings have confirmed that, levels of iNOS and $ONOO^-$ are consistently increased across different ICH models, such as the collagenase model (Chen et al., 2015; Kim et al., 2009; Wang and Dore, 2008; Wang et al., 2007), the autologous blood model (Zhao et al., 2007) and the single hemoglobin model (Ding et al., 2014; 2015). They also strongly suggest that excessive iNOS expression and $ONOO^-$ formation may be related to secondary brain injury following ICH. The differences observed in iNOS expression and $ONOO^-$ formation in the various ICH models lies mainly in the differences of their temporal and spatial profiles. Release of Hemoglobin (Hb) released from extravasated erythrocytes plays an important role in blood-brain barrier (BBB) disruption, edema formation, matrix metalloproteinase activation, NOS overexpression and excessive nitric oxide (NO) production after ICH (Huang et al., 2002; Katsu et al., 2010; Yang et al., 2013). Therefore, in this study, we used a hypertensive intracerebral hemorrhage (HICH) model in which hemorrhage was induced by Hb injection into the caudate nucleus of hypertensive rats. A previous study showed that levels of iNOS and 3-nitrotyrosine (3-NT), a reliable marker for the presence of $ONOO^-$, were significantly increased after Hb injection (Ding et al., 2014). iNOS was highly expressed in the microglia/macrophages, the presence of which typically indicates neuroinflammation. More importantly, levels of 3-NT in blood serum and brain tissues correlated with the severity of neurological deficits and with brain edema content. In this study, we investigated whether the protective effect of MSC transplantation involves inhibition of iNOS expression and $ONOO^-$ formation after HICH.

MATERIALS AND METHODS

Animals

Male spontaneously hypertensive rats, weighing 250-300 g, were purchased from the Animal Experiment Center of Charles River (China). Animals were maintained under a 12h light/ 12h dark cycle, with standard food and water. Animal experimental procedures were approved and regulated by the Institutional Animal Ethics Committee of Southern Medical University of China. All surgeries were performed under sodium pentobarbital anesthesia.

Generation, expansion and characterization of MSCs

Mesenchymal stromal cells were obtained from adult male spontaneously hypertensive rats weighing 80-120 g. Briefly, the femurs and tibias of the rats were collected under aseptic conditions. Then the cells were rinsed from the marrow cavity of the bones with 5 ml of DMEM/F-12 (1:1) medium using a 25-gauge needle. The cells were suspended in D-MEM/F-12 supplemented with 10% fetal bovine serum and cultured in 25 cm^2 culture flasks. After 72h of incubation at 37°C in a humidified atmosphere of 5% CO_2, non-adherent cells were removed, and fresh culture medium was added. When a confluence of 90% was reached, the remaining adherent cells were trypsinized, harvested and expanded. Cells from 3-5 generations were harvested for further testing or transplantation. Expression of the typical MSC markers CD29 (BD Pharmingen, USA), CD44 (BD Pharmingen, USA) and CD90 (BD Pharmingen, USA), and the absence of the hematopoietic markers CD45 (BD Pharmingen, USA), were assessed by flow cytometry analysis.

Surgical Procedure

All rats were randomly divided into three groups: (1) sham group; (2) HICH-vehicle group; (3) HICH-MSC group. Induction of HICH was performed as described previously (Yang et al., 2013). Briefly, after anesthetized and positioned, an incision was made along the sagittal midline to expose the skull using a sterile technique. After the cranial burr hole (1 mm) was drilled, a microsyringe was inserted stereotactically into the right caudate nucleus (3.4 mm lateral to the midline, 1 mm anterior to the coronal suture of the bregma, 6 mm below the surface of the skull), and then withdrawn 0.5 mm. Using a microinjection pump, 20 μl of hemoglobin (Hb; Sigma-Aldrich, USA) at a concentration of 150 mg/ml was injected into the nucleus over 10 min. Rats, in the sham group, were subjected to only a needle insertion using the same method. After injection, the needle was left in place for an additional 10 min to prevent any reflux and then slowly removed. The burr hole was sealed with bone wax, and the skin incision was closed. The animals were allowed to recover with free access to food and water for the duration of observation.

Labeling of MSCs and transplantation

After being trypsinized and washed with sterile phosphate-buffered saline (PBS), MSCs were labeled with the red fluorescent cell tracking dye Paul Karl Horan-26 (PKH26; Sigma, Aldrich) and the blue fluorescent cell tracking dye 4′,6-diamidino-2-phenylindole dihydrochloride (DAPI; Beyotime, China). Labeling was performed according to the manufacturer's instructions. After washing with PBS, MSCs were diluted to a concentration of 1×10^5 cells/μl with PBS. Six

hours after HICH, 10 μl of this solution were stereotaxically injected into three hematoma-correlated sites: (1) anterior-posterior (A-P), +2.5 mm; medial-lateral (M-L), -3.4 mm; dorsal-ventral (D-V) from the skull, -4.0 mm; (2) A-P, +1.0 mm; M-L, -3.4 mm; D-V from the skull, -4.0 mm; and (3) A-P, -0.5 mm; M-L, -3.4 mm; D-V from the skull, -4.0 mm, as previously reported (Liang et al., 2013). In the HICH-vehicle group, an equal volume of sterile PBS was administered to the same sites of rat brain.

Behavioral testing

Behavioral testing was conducted before Hb injection and at 3 and 7 days after Hb injection using the modified neurological severity score (mNSS) (Liao et al., 2009; Zhang et al., 2002) and the modified limb placing test (mLPT) (Hua et al., 2002). These tests were conducted by investigators who were blind to group allocation. The mNSS test (including motor, sensory, reflex and balance tests) is graded on a scale of 0-18, where a total score of 18 points indicates severe neurological deficit and a score of 0 indicates normal performance; 13-18 points indicates severe injury, 7-12 indicates moderate injury, and 1-6 indicates mild injury. The mLPT test was a vibrissae-elicited forelimb placing test. Independent testing of each forelimb was induced by brushing the respective vibrissae on the corner edge of a countertop. Intact animals place the forelimb ipsilateral to the stimulated vibrissae quickly onto the countertop. Depending on the extent of injury, the ability of the rat to place the forelimb contralateral to the injury in response to contralateral vibrissae contact with countertop may be impaired. In the experiments each rat was tested 10 times for each forelimb, and the percentage of trials in which the rat placed the appropriate forelimb on the edge of the countertop in response to the vibrissae stimulation was determined.

Imaging of PKH26-DAPI-labeled cells in the rat brain after HICH

After behavioral testing, animals were anesthetized and perfused through the heart with cold saline followed by 4% paraformaldehyde solution. After 24 h of fixation in 4% paraformaldehyde, the brains were fixed with 30% sucrose at 4°C for another 24 h and cut on a cryostat (Leica CM 1850UV) into 10-μm sections. Images were obtained with a confocal laser scanning microscope (FV10i-W, OLYMPUS).

Measurements of brain water content

Brain water content was measured 3 days after HICH. After anesthesia and decapitation, the brains were immediately extracted and the cerebella and brain stem were removed and then divided into two hemispheres along the midline. Ipsilateral and contralateral hemispheres were placed on a pre-weighed piece of aluminum foil to obtain the wet weight and then dried in an electric oven at 100°C for 24 h to obtain the dry weight. The brain water percentage was calculated using the formula: (wet weight - dry weight)/(wet weight) × 100.

Real-time quantitative polymerase chain reaction

Briefly, total RNA from rat brain tissue was extracted using the GeneJET™ RNA Purification Kit (Thermo Fisher Scientific, USA). The first strand cDNA was synthesized from RNA using the Maxima First Strand cDNA Synthesis Kit (Thermo Fisher Scientific). The primers for rat iNOS, ZO-1 and β-actin were designed using the Primer Premier 6.0 software (PREMIER Biosoft, Canada). The primers were: rat iNOS 5′-CGGAAGAGACGCACAGGCAGAGGTT-3′ (forward primer) and 5′-AAGGCAGCAGGCACACGCAATGATG-3′ (reverse primer); ZO-1 5′-GCTCACCAGGGTCAAAATGT-3′ (forward primer) and 5′-GGCTTAAAGCTGGCAGTGTC-3′ (reverse primer); β-actin 5′-CCACCCGCGAGTACAACCTTCTT-3′ (forward primer) and 5′-GAAGCCGGCCTTGCACATGCC-3′ (reverse primer). Primers were constructed by Life Technologies Corporation and polymerase chain reaction (PCR) reactions were run using the Power SYBR® Green PCR Master Mix (Life Technologies Corporation). The expression levels of target genes were calculated using the standard curve method. Fold changes in gene expression were evaluated compared to sham levels.

Enzyme-linked immunosorbent assay analysis

Brain tissues around the lesion sites were collected at specific time points (24 and 72 h after Hb injection, or the corresponding sham operation). Supernatants were extracted by homogenization and centrifugation (12,000 rpm for 15 min), and then stored at -80°C until use. Levels of interleukin 1 beta (IL-1β) and tumor necrosis factor alpha (TNF-α) were assayed using commercial enzyme-linked immunosorbent assay kits (Bio-Rad, USA) according to the manufacturer's instructions. Color intensities of samples were measured at 450 nm using an automatic microplate reader (Spectramax M5, Molecular Devices, USA).

Preparation of paraffin sections

After being anesthetized, animals were perfused through the heart with cold saline followed by 4% paraformaldehyde solution. Brain tissues were extracted and fixed by immersion in 4% paraformaldehyde solution at 4°C for 24 h. After being further dehydrated and vitrified, they were embedded in paraffin and cut into 5-μm sections. Before staining for H&E, immunofluorescence and immunohistochemistry, the sections were de-waxed and rehydrated in xylene, graded ethanol and then deionized water.

Immunofluorescence of iNOS, 3-NT and ZO-1

Antigen retrieval was performed by heat treatment in a microwave oven for 25 min in Tris-EDTA buffer solution (0.05 mol/L Tris, 0.001 mol/L EDTA; pH 8.5). In order to block the non-specific binding of primary antibodies, sections were incubated for 20 min in normal 5% bovine serum albumin. Subsequently, sections were incubated overnight at 4°C with primary antibody (rabbit polyclonal anti-iNOS, 1:50, Santa Cruz; mouse monoclonal anti-3-NT, 1:200, Abcam; mouse monoclonal anti-ZO-1, 1:100, Invitrogen). After being washed with PBS, sections were then incubated with the secondary antibody (Alexa Fluor 594 donkey anti-mouse IgG, 1:100, Invitrogen; Alexa Fluor 488 donkey anti-rabbit IgG, 1:100, Invitrogen) for 1 h at 37°C. For double-staining experiments, primary antibodies were mixed and incubated overnight at

4°C. Nuclei were stained by Hoechst 33342 (Sigma-Aldrich) for 10 min at room temperature. Images were obtained with a fluorescence microscope (Bx51; OLYMPUS). Image processing was performed with the use of Photoshop CS5 software (Adobe Systems Incorporated, USA).

Immunohistochemical measurement of CD68, Iba1 and NeuN

For antigen retrieval, slides were boiled in a microwave oven for 25 min in 0.01 mol/L citrate buffer solution (pH 6.0). Endogenous peroxidase activity was blocked using 0.3% H_2O_2 for 10 min followed by washing with PBS. After blocking in goat serum for 15 min, sections were incubated overnight at 4°C with primary antibody (mouse monoclonal anti-CD68, 1:100, Santa Cruz; goat polyclonal anti-Iba1, 1:400, Abcam; mouse monoclonal anti-NeuN, 1:300, Abcam). After washing with PBS, sections were incubated with biotinylated goat anti-mouse or rabbit anti-goat IgG secondary antibody for 15 min and then incubated with horseradish peroxidase streptavidin reagent for 15 min. Finally, immunoreactivity was detected using 3, 3′-diaminobenzidine (DAB; Boster), followed by restaining with hematoxylin. Images were obtained with the use of a microscope (Bx51; OLYMPUS).

Terminal deoxynucleotidyl transferase-mediated deoxyuridine triphosphate nick-end labeling (TUNEL) assay

The TUNEL was performed to detect dying cells using the In Situ Cell Detection Kit (Roche, USA) according to the manufacturer's instructions. Sections from the same brain sites or areas described above were selected for TUNEL assay. The number of positive cells near the injured areas was counted by an experimenter blind to the group assignment of the samples.

Statistical analysis

All data are presented as mean ± standard deviation (SD). Statistical analysis was performed using the SPSS 13.0 software (USA). Comparisons between groups were determined by Student's *t* test or one-way analysis of variance (ANOVA) and followed by LSD and Dunnett's T3 tests for the two groups' comparison within the multiple groups. Differences were considered significant for $p < 0.05$.

RESULTS

Characterization of MSCs

Mesenchymal stromal cells were adherent and bipolar spindle-like in standard culture conditions (Fig. 1A). Flow cytometric analysis demonstrated that MSCs expressed CD90 (100.00%), CD29 (100.00%) and CD44 (99.24%), but did not express CD45 (0.26%) (Figs. 1B and 1C). This suggests that a high purity culture of MSCs was obtained.

Survival of transplanted MSCs

MSCs were labeled with the red fluorescent cell tracking dye PKH26 and the blue fluorescent cell tracking dye DAPI. Labeled MSCs were transplanted into the perilesional region 6 h after HICH at three hematoma-correlated sites. At 3 days post-HICH, rats were euthanized to analyze the transplanted MSCs *in vivo*. There was no tumor formation or uncontrolled graft growth observed in the brains of the MSC group. We observed large numbers of PKH26/DAPI-double-positive cells in the injured hemisphere (Fig. 1D).

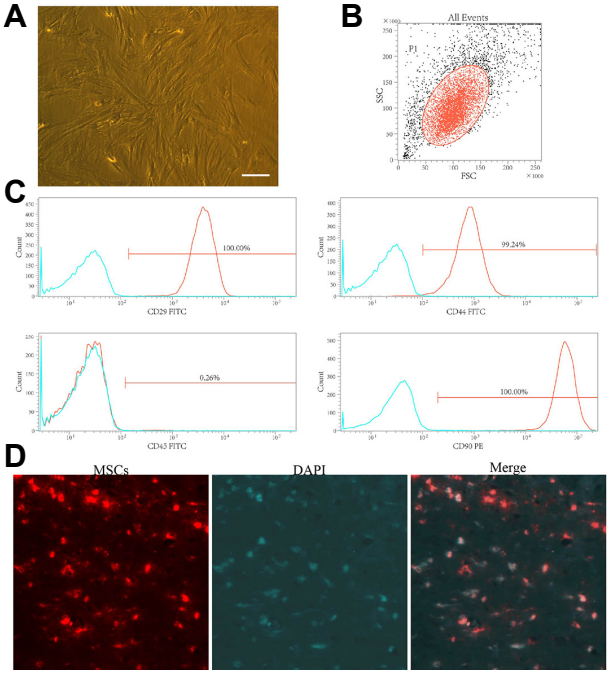

Fig. 1. Characterization of MSCs. (A) Morphology of MSCs. Scale bar: 200 μm. (B, C) Analysis of surface marker expression in MSCs performed by flow cytometry showed high positivity for CD44 (99.24%), CD90 (99.98%) and CD29 (99.92%), but low positivity for CD45 (0.26%). (D) Survival of MSCs in the rat brain after HICH. Cells doubly-labelled with PKH26/DAPI were observed in the lesion site 3 days after HICH. Original magnification: ×400.

Treatment with MSCs improved neurological recovery after HICH

In order to assess the effects of administration of MSCs after HICH, the mNSS and mLPT were performed at 24 h and 72 h post-HICH (Fig. 2A). The results of the mNSS test showed that Hb-injected rats exhibited significant neurological deficits at 24 and 72 h. Treatment with MSCs moderately reduced the neurological impairments at 24 h but showed no significant difference ($p = 0.059$). At 72 h, the neurological deficits measured by the mNSS test were significantly ameliorated by MSCs treatment ($p < 0.01$). In the mLPT score, there was a significant improvement in neurological function in the MSC-treated group compared with the vehicle group both at 24 h ($p < 0.05$) and 72 h ($p < 0.05$) post-HICH.

Treatment with MSCs reduced brain water content after HICH

To investigate whether MSCs could attenuate brain edema, we monitored brain water content in the experimental

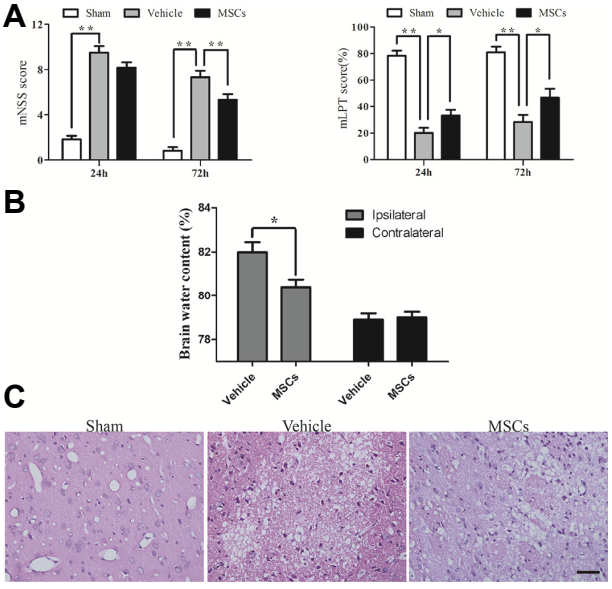

Fig. 2. Improvement of neurological function and alteration of brain water content after MSC treatment. (A) Rats receiving MSC transplantation showed significant recovery of neurological function on the mNSS and mLPT tests compared to the HICH-vehicle group at 24 h and/or 72 h (n = 6). (B) Brain water content was also reduced in the lesioned hemisphere in the HICH-MSC group compared to the HICH-vehicle group at 3 days (n = 4). (C) H&E staining likewise showed that the HICH-MSC group had lower brain water content at 3 days. ** $p < 0.01$; * $p < 0.05$. Scale bar: 50 μm.

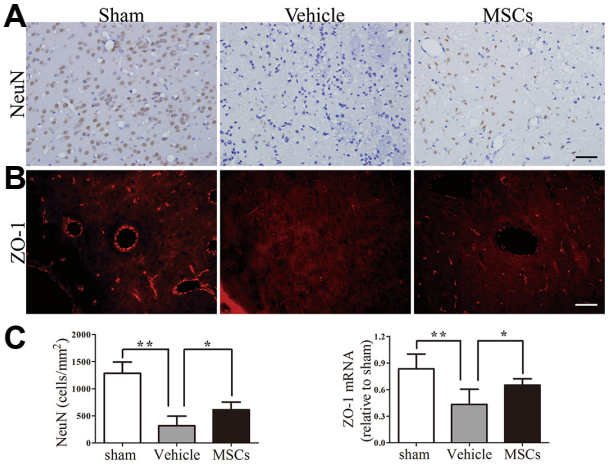

Fig. 3. Neural protection and alterations to tight junction expression after treatment. (A) Transplantation of MSCs increased the number of NeuN+ cells in the perihematomal region. (B) Brain sections from the sham group, HICH-vehicle group and HICH-MSC group were analyzed for ZO-1 by a fluorescence microscope at 3 days following HICH. Increased intensity of ZO-1 expression was observed in the HICH-MSC group compared with the HICH-vehicle group. (C) Quantification of cell marker expression showed a significant increase in the number of NeuN+ cells (n = 4) and the mRNA expression levels of ZO-1 in the HICH-MSC group at 3 days (n = 5), compared with the HICH-vehicle group. ** $p < 0.01$; * $p < 0.05$. Scale bar: 50 μm.

groups 3 days post-HICH. Brain water content on the ipsilateral side to the injury was significantly lower in HICH-MSC group than in the HICH-vehicle group (80.41 ± 0.69% vs. 81.99 ± 0.91%, $p < 0.05$). However, the contralateral brain water content in both groups did not differ (79.00 ± 0.52% vs. 78.90 ± 0.58%, $p = 0.805$) (Fig. 2B). Staining with H&E also confirmed that MSCs attenuated brain edema after HICH (Fig. 2C).

Neuroprotection by MSCs

To determine the survival of neurons, immunohistochemistry was performed to detect the expression of NeuN protein. The HICH-MSC group exhibited a significantly higher number of NeuN+ cells (NeuN+: 440.77 ± 73.53 cells/mm^2) compared to the HICH-vehicle group (NeuN+: 187.67 ± 136.86 cells/mm^2; $p < 0.05$; Figs. 3A and 3C).

Alterations of ZO-1 protein expression after Hb injection

To evaluate the effect of MSCs on endothelial tight junctions of the BBB after HICH, we examined the expression of ZO-1 using immunofluorescence and PCR. In sham control rats (Fig. 3B), intact ZO-1 expression was observed to be distributed in a continuous and linear pattern. Compared with the HICH-vehicle group, ZO-1 staining in the HICH-MSCs group was increased but still appeared slightly diffuse and discontinuous. The mRNA level of ZO-1 was also markedly decreased in the injured region compared to the sham-operated groups ($p < 0.01$; Fig. 3C). Administration of MSCs significantly ameliorated the Hb-mediated decrease in expression of ZO-1 relative to the HICH-vehicle group ($p < 0.05$).

Treatment with MSCs decreased Iba1-positive, CD68-positive and apoptotic cell numbers

Microglial activation is an important feature of the pathological changes that follow ICH. In MSC-treated rats, microglial activation, as shown by Iba1 (Figs. 4A and 4C) and CD68 (Figs. 4B and 4D) immunostaining, was substantially attenuated at 3 days post-transplantation compared with the HICH-vehicle group. The number of Iba1-positive cells around the hematoma in the HICH-MSC group and HICH-vehicle group were 552.69 ± 87.91 vs. 991.74 ± 211.30 cells/mm^2 ($p < 0.05$), respectively, whereas CD68-positive cell number in the two groups were 339.19 ± 133.35 vs. 642.22 ± 138.24 cells/mm^2 ($p < 0.05$), respectively. To assess the effects of MSCs on apoptosis, we measured the number of TUNEL-immunopositive cells (Figs. 6A and 6B). The number of apoptotic cells was significantly increased at 3 days after Hb injection compared to sham group (554.41 ± 113.81 vs. 26.4 ± 14.72 cells/mm^2; $P < 0.01$), but MSC administration significantly reduced apoptotic cell numbers relative to the HICH-Vehicle group (336.32 ± 127.54 vs. 554.41 ± 113.81 cells/mm^2; $p < 0.05$).

Treatment with MSCs reduced the levels of IL-1β and TNF-α

To investigate the anti-inflammatory effects of MSCs, we

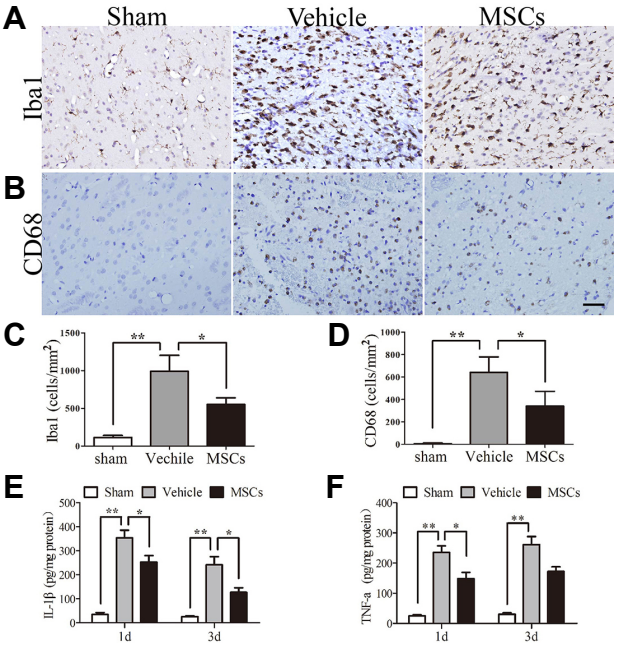

Fig. 4. Effect of MSCs on the expression of Iba1, CD68, IL-1β and TNF-α in ipsilateral rat brain post-HICH. (A, B) Photomicrographs showed decreased expression of Iba-1 and CD68 in the HICH-MSC group compared to the HICH-vehicle group. The sham group had few Iba1 and CD68 positive cells. In contrast, increased levels of Iba1 and CD68 were detected at 3 days post-HICH in the HICH-vehicle group, with a significant reduction of Iba1 and CD68 levels observed after MSC injection. (C, D) Quantification of Iba1 and CD68 levels in the different groups. (E, F) Levels of the proinflammatory cytokines IL-1β and TNF-α were decreased in the MSC-treated group at 1 and 3 days, compared with the HICH-vehicle group. $**p < 0.01$; $*p < 0.05$; n = 4 per group. Scale bar: 50 μm.

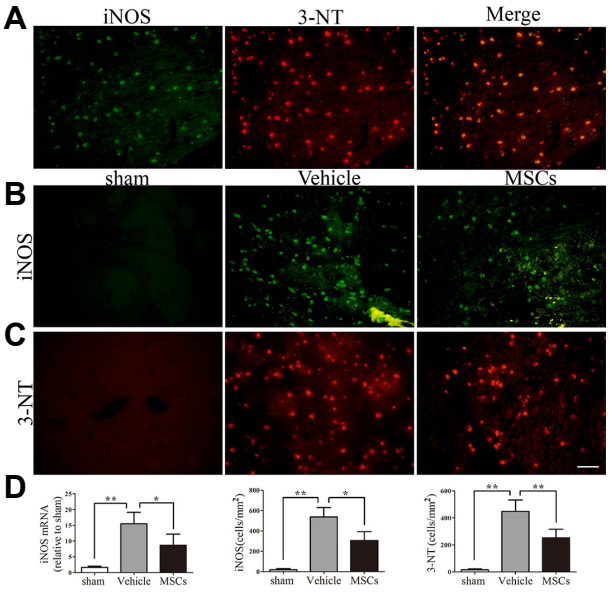

Fig. 5. Effect of MSCs on iNOS and 3-NT expression in the ipsilateral brain hemisphere at 24 hours post-HICH. (A) In the HICH-vehicle group, enhanced expression of iNOS (green) and 3-NT (red) was detected in the brain hemisphere ipsilateral to the injury. Colocalized expression of iNOS and 3-NT as a yellow-red fluorescence confirms that $ONOO^-$ is mainly produced by iNOS. (B) Photomicrographs showed enhanced expression of iNOS (green) in the HICH-vehicle group compared to the HICH-MSC group. The sham group showed very few iNOS positive cells. (C) The more intense red fluorescence in HICH-vehicle sections indicated a higher immunoreactivity for 3-NT compared to sham, while MSC-treated animals had reduced expression of 3-NT relative to HICH-vehicle. (D) Quantification of iNOS and 3-NT levels by PCR (n = 5 per group) and immunofluorescence (n = 4 per group) for the different groups. $**p < 0.01$; $*p < 0.05$; Scale bar: 50 μm.

measured the levels of pro-inflammatory factors (IL-1β and TNF-α) in the injured hemisphere. Compared with the HICH-Vehicle group, the levels of IL-1β were significantly decreased after MSCs treatment at 24 h ($p < 0.05$; 353.35 ± 78.80 vs. 252.20 ± 66.14 pg/mg protein) and 72 h ($p < 0.05$, 241.65 ± 82.27 vs. 126.57 ± 46.80 pg/mg protein) (Fig. 4E). Similarly, the level of TNF-α was evidently reduced at 24 h after Hb injection compared with the sham-operated group ($p < 0.05$; 235.58 ± 52.52 vs. 148.12 ± 51.25 pg/mg protein) (Fig. 4F). At 72 h, the level of TNF-α was seemingly lower in the MSC-treated group than in the HICH-Vehicle group but showed no significant difference ($p = 0.057$; 261.00 ± 65.77 vs. 172.13 ± 37.48 pg/mg protein).

Treatment with MSCs decreased iNOS-positive and 3-NT-positive cell numbers

Due to the instability of peroxynitrite, its detection through 3-NT formation is a marker of the levels of $ONOO^-$. By double-staining for iNOS and 3-NT, we further identified that they were colocalized after HICH, suggesting that $ONOO^-$ production comes mainly from the expression or activation of iNOS (Fig. 5A). As is shown in Fig. 5B, iNOS immunoreactivity was increased in peri-ICH regions in the HICH-vehicle group compared to sham ($p < 0.01$; 537.19 ± 91.88 vs. 18.94 ± 11.76 cell/mm^2; Fig. 5D), but it was significantly attenuated in the HICH-MSC group compared to the HICH-vehicle group ($p < 0.05$; 304.75 ± 88.26 cell/mm^2). Similarly, expression of iNOS mRNA was significantly decreased in the HICH-MSC group compared to the HICH-vehicle group ($p < 0.05$; Fig. 5D). Furthermore, in a matching pattern to that observed for iNOS expression, 3-NT immunoreactivity significantly increased in the peri-HICH region in the HICH-vehicle group compared to sham ($p < 0.01$; 447.66 ± 84.72 vs. 15.50 ± 6.60 cell/mm^2). Moreover, treatment with MSCs significantly ameliorated the number of 3-NT-positive cells relative to the HICH-vehicle group ($p < 0.01$; 251.38 ± 65.22 cell/mm^2) (Figs. 5C and 5D).

DISCUSSION

Inflammation plays an important role in pathological pro-

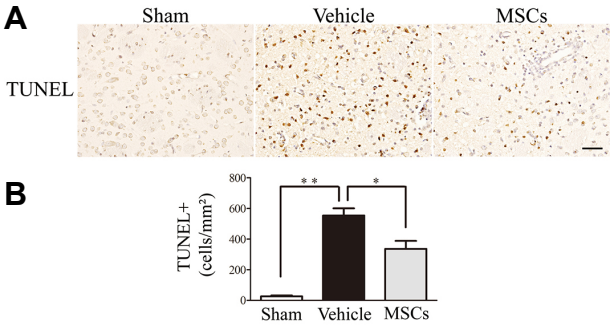

Fig. 6. Effect of MSC treatment on cell apoptosis in the ipsilateral brain hemisphere at 3 days post-HICH. (A) Cell apoptosis was determined by TUNEL assay. (B) The number of apoptotic cells in the injured striata at 3 days after Hb injection was significantly reduced in the HICH-MSC group compared to the HICH-vehicle group (n = 4 per group). $*p < 0.05$; $**p < 0.01$. Scale bar: 50 μm.

cesses following ICH-induced brain injury. Indeed, Gong et al. confirmed that the inflammatory reaction induced by toxic blood components contributes to secondary brain injury after ICH (Gong et al., 2000). Currently, stem cells are becoming more and more promising as a therapeutic strategy for treating nervous system injury. Mesenchymal stromal cells, which are known to be self-renewing and pluripotent, are capable of differentiating into osteoblasts, chondrocytes, adipocytes, muscle cells, neurons and glial cells *in vitro* and *in vivo* (Hermann et al., 2004; Jiang et al., 2002; Liang et al., 2013; Liao et al., 2009; Nagai et al., 2007; Pittenger et al., 1999), promoting the repair of tissue damage. Moreover, owing to their limited immunogenicity, MSCs are immunoprivileged, thereby allowing them to be used in allogenous or xenogenous conditions. Indeed, MSCs are able to maintain the resting phenotype of microglia and inhibit microglial activation (Yan et al., 2013). In this study, following their administration to treat Hb-induced HICH rats, MSCs were found to reduce hemispheric water content, perihematomal neuronal death and cell apoptosis. Furthermore, they decreased infiltration of microglia and pro-inflammatory cytokines, as well as iNOS expression and $ONOO^-$ formation, and increased ZO-1 expression in perihematomal regions. Concomitant with these changes, they also improved the functional outcome. Our data provide initial evidence that MSCs modulate inflammation against HICH via inhibition of iNOS expression and $ONOO^-$ formation.

Improvements in both behavior and the number of cells surviving post-graft are important measures of treatment efficacy following stem cell-based cell therapy in ICH animal models (Nagai et al., 2007). To visualize MSCs accurately in vivo, we used both a red membrane labeling fluorescent dye, PKH26, and a blue fluorescent cell tracking dye, DAPI, as tracers. The use of the nontoxic dye PKH26 as a marker for identifying transplanted cells in vivo is well-established (Jin et al., 2011; Liang et al., 2013). The fluorescent DNA dye DAPI has been used extensively for visualizing cell nuclei and is commonly used in immunocytochemistry applications, without changing cell viability and proliferation of MSCs (Ocarino et al., 2008). In the present study, large numbers of PKH26/DAPI double-positive cells were observed in the injured hemisphere, which indicates that transplanted MSCs were able to survive in vivo for at least 3 days.

A reduction in blood flow after ICH results in damage to neuronal networks and the impairment of neural function. Synaptic and network level plasticity are crucial for functional compensation during stroke recovery (Murphy and Corbett, 2009). Interestingly, transplantation of bone marrow stromal cells significantly enhanced neuronal plasticity of the denervated corticospinal tract at bilateral forelimb areas of the cortex after ICH (Liang et al., 2013). In the present study, our results also suggest that intracerebral injection of MSCs was able to improve the survival of neurons and neural function.

Disruption of the BBB is a prominent feature of ICH (Yang et al., 2013), with reports suggesting that injection of lysed erythrocytes induces a significant increase in BBB leakage and brain water content after 24 h (Bhasin et al., 2002; Xi et al., 1998; 2001). To investigate whether transplanted MSCs were capable of reducing brain water content and protect BBB, immunofluorescence and PCR of ZO-1 was performed. The peripheral tight junction protein ZO-1 is found on epithelial and endothelial cell membranes, and its loss increases BBB permeability (Yang et al., 2013). In the present study, both protein and mRNA levels of ZO-1 were significantly increased in the perihematomal region after MSC treatment. Meanwhile, brain water content was also significantly reduced in the HICH-MSC group. This indicates that MSCs may have a role in protecting the integrity of the BBB, a finding that is in agreement with the results of previous studies (Zhang et al., 2013).

Inflammatory cell infiltration and microglial activation following ICH increases the production of inflammatory substances, such as proinflammatory cytokines, cyclooxygenase-2, and iNOS (Nogawa et al., 1998; Pacher et al., 2007). Inhibition of these inflammatory substances contributes to reducing brain edema and cell death, and improves functional outcome after ICH (Jung et al., 2004). Interestingly, MSCs have been shown to decrease proinflammatory cytokine secretion, leukocyte infiltration, and microglial activation. They also reduce levels of reactive oxygen species (ROS), production of MMPs, and upregulate IL-6, IL-10 and transforming growth factor beta (TGF-β) expression (Chen et al., 2015; Di Nicola et al., 2002; Liao et al., 2009; Meirelles et al., 2009; Yan et al., 2013; Zhang et al., 2013). In the current study we observed that after MSC treatment, microglial activation, visualized by CD68 and Iba-1 immunostaining, was substantially attenuated and levels of pro-inflammatory cytokines (such as IL-1β and TNF- α) were significantly decreased, in line with the studies cited above. Moreover, we noted in particular that MSCs partially inhibited iNOS expression and $ONOO^-$ formation in HICH.

Increasing iNOS and $ONOO^-$ levels contribute to the inflammatory response and accelerate oxidative/nitrative stress injury in the brain following ICH (Pacher et al., 2007). Under various pathological statuses associated with inflammation, such as cerebral ischemia, the expression of iNOS causes large amounts of NO to be produced in the brain, which can result in a variety of deleterious effects (Moncada and Bo-

lanos, 2006; Pacher et al., 2007). The iNOS-derived NO can activate MMP-9, facilitating neuroinflammation and contributing to disruption of the BBB (Pannu and Singh, 2006; Tejima et al., 2007; Wu et al., 2011). After ICH, iNOS levels are also dramatically increased (Yang et al., 2013; Zhao et al., 2007). Notably, Kim et al. found that iNOS knockout mice had significantly less brain edema than controls (Kim et al., 2009). Furthermore, there is evidence showing that inhibition of iNOS contributes to a reduction in the inflammatory response and improves functional outcomes in experimentally-induced ICH (Jung et al., 2004; Nogawa et al., 1998; Wu et al., 2011). Similarly, in our experiment, iNOS expression was decreased in perihematomal regions of HICH rats following MSC treatment, and accompanied by a subsequent partial recovery of neurological function.

Peroxynitrite is a strong oxidizing and nitrating agent (Beckman and Koppenol, 1996; Pacher et al., 2007a), which is mainly generated by iNOS (Hirabayashi et al., 2000), as also demonstrated in this study (Fig. 5A). The production of $ONOO^-$ is very low under physiological conditions, while under pathological conditions, the rate of formation of $ONOO^-$ from superoxide and NO dramatically increases. Excessive $ONOO^-$ will result in substantial oxidation and destruction of cellular constituents, leading to serious consequences, such as the dysfunction of cell signaling pathways, critical cellular processes, and the induction of cell death or apoptosis (Pacher et al., 2007; Virag et al., 2003). There is evidence showing that the decomposition of $ONOO^-$ decreases MMP activation, brain edema and neurovascular injury in a rat model of experimental stroke (Khan et al., 2012; Suofu et al., 2010). In our experiment, $ONOO^-$ was decreased in the perihematomal region following MSC treatment. Therefore, we speculate that MSCs might attenuate neuronal injury, brain edema and apoptopic cell numbers in the perihematomal penumbra by reducing the production of iNOS and $ONOO^-$.

In conclusion, we have provided convincing evidence that MSC transplantation has beneficial effects in hemoglobin-induced HICH by improving neural function, relieving disruption of the BBB, reducing brain edema and decreasing cell apoptosis. The potential mechanism for these effects may involve the suppression of iNOS expression and subsequent $ONOO^-$ formation. Therefore, increasing our understanding of the mechanisms underlying the anti-inflammatory and neuroprotective effects of MSCs may help to bring us new treatment strategies for HICH.

ACKNOWLEDGMENTS

This study was supported by the Key Science and Technology Project of Jingmen City, HuBei Province (No. YFZD2016045). The work of flow cytometry was supported by Guangdong Provincial Key Laboratory of Malignant Tumor Epigenetics and Gene Regulation, Sun Yat-Sen Memorial Hospital, Sun Yat-Sen University.

REFERENCES

Aronowski, J., and Hall, C.E. (2005). New horizons for primary intracerebral hemorrhage treatment: experience from preclinical studies. Neurol Res. *27*, 268-279.

Balami, J.S., and Buchan, A.M. (2012). Complications of intracerebral haemorrhage. Lancet Neurol. *11*, 101-118.

Beckman, J.S., and Koppenol, W.H. (1996). Nitric oxide, superoxide, and peroxynitrite: the good, the bad, and ugly. Am. J. Physiol. *271*, C1424-1437.

Bhasin, R.R., Xi, G., Hua, Y., Keep, R.F., and Hoff, J.T. (2002). Experimental intracerebral hemorrhage: effect of lysed erythrocytes on brain edema and blood-brain barrier permeability. Acta Neurochir. Suppl. *81*, 249-251.

Candelise, L., Gattinoni, M., Bersano, A., Micieli, G., Sterzi, R., and Morabito, A. (2007). Stroke-unit care for acute stroke patients: an observational follow-up study. Lancet *369*, 299-305.

Chen, M., Li, X., Zhang, X., He, X., Lai, L., Liu, Y., Zhu, G., Li, W., Li, H., Fang, Q., Wang, Z., and Duan, C. (2015). The inhibitory effect of mesenchymal stem cell on blood-brain barrier disruption following intracerebral hemorrhage in rats: contribution of TSG-6. J. Neuroinflammation *12*, 61.

Di Nicola, M., Carlo-Stella, C., Magni, M., Milanesi, M., Longoni, P.D., Matteucci, P., Grisanti, S., and Gianni, A.M. (2002). Human bone marrow stromal cells suppress T-lymphocyte proliferation induced by cellular or nonspecific mitogenic stimuli. Blood *99*, 3838-3843.

Ding, R., Chen, Y., Yang, S., Deng, X., Fu, Z., Feng, L., Cai, Y., Du M, Zhou, Y., and Tang, Y. (2014). Blood-brain barrier disruption induced by hemoglobin *in vivo*: Involvement of up-regulation of nitric oxide synthase and peroxynitrite formation. Brain Res. *1571*, 25-38.

Ding, R., Feng, L., He, L., Chen, Y., Wen, P., Fu, Z., Lin, C., Yang, S., Deng, X., Zeng, J., and Sun, G. (2015). Peroxynitrite decomposition catalyst prevents matrix metalloproteinase-9 activation and neurovascular injury after hemoglobin injection into the caudate nucleus of rats. Neuroscience *297*, 182-193.

Fatar, M., Stroick, M., Griebe, M., Marwedel, I., Kern, S., Bieback, K., Giesel, F.L., Zechmann, C., Kreisel, S., Vollmar, F., et al., (2008). Lipoaspirate-derived adult mesenchymal stem cells improve functional outcome during intracerebral hemorrhage by proliferation of endogenous progenitor cells stem cells in intracerebral hemorrhages. Neurosci Lett. *443*, 174-178.

Gong, C., Hoff, J.T., and Keep, R.F. (2000). Acute inflammatory reaction following experimental intracerebral hemorrhage in rat. Brain Res. *871*, 57-65.

Hermann, A., Gastl, R., Liebau, S., Popa, M.O., Fiedler, J., Boehm, B.O., Maisel, M., Lerche, H., Schwarz, J., Brenner, R., et al. (2004). Efficient generation of neural stem cell-like cells from adult human bone marrow stromal cells. J. Cell Sci. *117*, 4411-4422.

Hirabayashi, H., Takizawa, S., Fukuyama, N., Nakazawa, H., and Shinohara, Y. (2000). Nitrotyrosine generation via inducible nitric oxide synthase in vascular wall in focal ischemia-reperfusion. Brain Res. *852*, 319-325.

Hua, Y., Schallert, T., Keep, R.F., Wu, J., Hoff, J.T., and Xi, G. (2002). Behavioral tests after intracerebral hemorrhage in the rat. Stroke *33*, 2478-2484.

Huang, F.P., Xi, G., Keep, R.F., Hua, Y., Nemoianu, A., and Hoff, J.T. (2002). Brain edema after experimental intracerebral hemorrhage: role of hemoglobin degradation products. J. Neurosurg. *96*, 287-93.

Jiang, Y., Jahagirdar, B.N., Reinhardt, R.L., Schwartz, R.E., Keene, C.D., Ortiz-Gonzalez, X.R., Reyes, M., Lenvik, T., Lund, T., Blackstad, M., et al. (2002). Pluripotency of mesenchymal stem cells derived from adult marrow. Nature *418*, 41-49.

Jin, S.Z., Meng, X.W., Sun, X., Han, M.Z., Liu, B.R., Wang, X.H., and Pei, F.H. (2011). Hepatocyte growth factor promotes liver regeneration induced by transfusion of bone marrow mononuclear cells in a murine acute liver failure model. J. Hepatobiliary Pancreat. Sci. *18*,

397-405.

Jung, K.H., Chu, K., Jeong, S.W., Han, S.Y., Lee, S.T., Kim, J.Y., Kim, M., and Roh, J.K. (2004). HMG-CoA reductase inhibitor, atorvastatin, promotes sensorimotor recovery, suppressing acute inflammatory reaction after experimental intracerebral hemorrhage. Stroke *35*, 1744-9.

Katsu, M., Niizuma, K., Yoshioka, H., Okami, N., Sakata, H., and Chan, P.H. (2010). Hemoglobin-induced oxidative stress contributes to matrix metalloproteinase activation and blood-brain barrier dysfunction in vivo. J. Cereb. Blood Flow Metab. *30*, 1939-1950.

Khan, M., Dhammu, T.S., Sakakima, H., Shunmugavel, A., Gilg, A.G., Singh, A.K., and Singh, I. (2012). The inhibitory effect of S-nitrosoglutathione on blood-brain barrier disruption and peroxynitrite formation in a rat model of experimental stroke. J. Neurochem. *123* Suppl 2, 86-97.

Kim, D.W., Im, S.H., Kim, J.Y., Kim, D.E., Oh, G.T., and Jeong, S.W. (2009). Decreased brain edema after collagenase-induced intracerebral hemorrhage in mice lacking the inducible nitric oxide synthase gene. Laboratory investigation. J. Neurosurg. *111*, 995-1000.

Liang, H., Yin, Y., Lin, T., Guan, D., Ma, B., Li, C., Wang, Y., and Zhang, X. (2013). Transplantation of bone marrow stromal cells enhances nerve regeneration of the corticospinal tract and improves recovery of neurological functions in a collagenase-induced rat model of intracerebral hemorrhage. Mol. Cells *36*, 17-24.

Liao, W., Zhong, J., Yu, J., Xie, J., Liu, Y., Du L, Yang, S., Liu, P., Xu, J., Wang, J., Han, Z., and Han, Z.C. (2009). Therapeutic benefit of human umbilical cord derived mesenchymal stromal cells in intracerebral hemorrhage rat: implications of anti-inflammation and angiogenesis. Cell. Physiol. Biochem. *24*, 307-316.

Masada, T., Hua, Y., Xi, G., Yang, G.Y., Hoff, J.T., and Keep, R.F. (2001). Attenuation of intracerebral hemorrhage and thrombin-induced brain edema by overexpression of interleukin-1 receptor antagonist. J. Neurosurg. *95*, 680-686.

Meirelles, L.S., Fontes, A.M., Covas, D.T., and Caplan, A.I. (2009). Mechanisms involved in the therapeutic properties of mesenchymal stem cells. Cytokine Growth Factor Rev. *20*, 419-427.

Moncada, S., and Bolanos, J.P. (2006). Nitric oxide, cell bioenergetics and neurodegeneration. J. Neurochem. *97*, 1676-1689.

Murphy, T.H., and Corbett, D. (2009). Plasticity during stroke recovery: from synapse to behaviour. Nat. Rev. Neurosci. *10*, 861-872.

Nagai, A., Kim, W.K., Lee, H.J., Jeong, H.S., Kim, K.S., Hong, S.H., Park, I.H., and Kim, S.U. (2007). Multilineage potential of stable human mesenchymal stem cell line derived from fetal marrow. PLoS One *2*, e1272.

Nogawa, S., Forster, C., Zhang, F., Nagayama, M., Ross, M.E., and Iadecola, C. (1998). Interaction between inducible nitric oxide synthase and cyclooxygenase-2 after cerebral ischemia. Proc. Natl. Acad. Sci. USA *95*, 10966-10971.

Ocarino, N.M., Bozzi, A., Pereira, R.D., Breyner, N.M., Silva, V.L., Castanheira, P., Goes, A.M., and Serakides, R., (2008). Behavior of mesenchymal stem cells stained with 4', 6-diamidino-2-phenylindole dihydrochloride (DAPI) in osteogenic and non osteogenic cultures. Biocell *32*, 175-183.

Pacher, P., Beckman, J.S., and Liaudet, L. (2007). Nitric oxide and peroxynitrite in health and disease. Physiol. Rev. *87*, 315-424.

Pannu, R., and Singh, I., (2006). Pharmacological strategies for the regulation of inducible nitric oxide synthase: neurodegenerative versus neuroprotective mechanisms. Neurochem. Int. *49*, 170-182.

Pittenger, M.F., Mackay, A.M., Beck, S.C., Jaiswal, R.K., Douglas, R., Mosca, J.D., Moorman, M.A., Simonetti, D.W., Craig, S., and Marshak, D.R. (1999). Multilineage potential of adult human mesenchymal stem cells. Science *284*, 143-147.

Qureshi, A.I., Mendelow, A.D., and Hanley, D.F. (2009). Intracerebral haemorrhage. Lancet *373*, 1632-1644.

Seyfried, D.M., Han, Y., Yang, D., Ding, J., Shen, L.H., Savant-Bhonsale, S., and Chopp, M. (2010). Localization of bone marrow stromal cells to the injury site after intracerebral hemorrhage in rats. J. Neurosurg. *112*, 329-335.

Steinberg, G.K., Kondziolka, D., Wechsler, L.R., Lunsford, L.D., Coburn, M.L., Billigen, J.B., Kim, A.S., Johnson, J.N., Bates, D., King, B., et al. (2016). Clinical outcomes of transplanted modified bone marrow-derived mesenchymal stem cells in stroke: a phase 1/2a study. Stroke *47*, 1817-1824.

Suofu, Y., Clark, J., Broderick, J., Wagner, K.R., Tomsick, T., Sa, Y., and Lu, A. (2010). Peroxynitrite decomposition catalyst prevents matrix metalloproteinase activation and neurovascular injury after prolonged cerebral ischemia in rats. J. Neurochem. *115*, 1266-1276.

Tejima, E., Zhao, B.Q., Tsuji, K., Rosell, A., van Leyen, K., Gonzalez, R.G., Montaner, J., Wang, X., and Lo, E.H., (2007). Astrocytic induction of matrix metalloproteinase-9 and edema in brain hemorrhage. J. Cereb. Blood Flow Metab. *27*, 460-468.

Vaquero, J., Otero, L., Bonilla, C., Aguayo, C., Rico, M.A., Rodriguez, A., and Zurita, M. (2013). Cell therapy with bone marrow stromal cells after intracerebral hemorrhage: impact of platelet-rich plasma scaffolds. Cytotherapy *15*, 33-43.

Virag, L., Szabo, E., Gergely, P., and Szabo, C. (2003). Peroxynitrite-induced cytotoxicity: mechanism and opportunities for intervention. Toxicol. Lett. *140-141*, 113-124.

Wang, J., and Dore, S. (2008). Heme oxygenase 2 deficiency increases brain swelling and inflammation after intracerebral hemorrhage. Neuroscience *155*, 1133-1141.

Wang, J., Fields, J., Zhao, C., Langer, J., Thimmulappa, R.K., Kensler, T.W., Yamamoto, M., Biswal, S., and Dore, S. (2007). Role of Nrf2 in protection against intracerebral hemorrhage injury in mice. Free Radic. Biol. Med. *43*, 408-414.

Wang, S.P., Wang, Z.H., Peng, D.Y., Li, S.M., Wang, H., and Wang, X.H. (2012). Therapeutic effect of mesenchymal stem cells in rats with intracerebral hemorrhage: reduced apoptosis and enhanced neuroprotection. Mol. Med. Rep. *6*, 848-854.

Wu, B., Ma, Q., Suzuki, H., Chen, C., Liu, W., Tang, J., and Zhang, J. (2011). Recombinant osteopontin attenuates brain injury after intracerebral hemorrhage in mice. Neurocrit. Care *14*, 109-117.

Xi, G., Keep, R.F., and Hoff, J.T. (1998). Erythrocytes and delayed brain edema formation following intracerebral hemorrhage in rats. J. Neurosurg. *89*, 991-6.

Xi, G., Hua, Y., Bhasin, R.R., Ennis, S.R., Keep, R.F., and Hoff, J.T. (2001). Mechanisms of edema formation after intracerebral hemorrhage: effects of extravasated red blood cells on blood flow and blood-brain barrier integrity. Stroke *32*, 2932-2938.

Yan, K., Zhang, R., Sun, C., Chen, L., Li, P., Liu, Y., Peng, L., Sun, H., Qin, K., Chen, F., et al. (2013). Bone marrow-derived mesenchymal stem cells maintain the resting phenotype of microglia and inhibit microglial activation. PLoS One *8*, e84116.

Yang, S., Chen, Y., Deng, X., Jiang, W., Li, B., Fu, Z., Du, M., and Ding, R. (2013). Hemoglobin-induced nitric oxide synthase overexpression and nitric oxide production contribute to blood-brain barrier disruption in the rat. J. Mol. Neurosci. *51*, 352-363.

Zhang, L., Schallert, T., Zhang, Z.G., Jiang, Q., Arniego, P., Li, Q., Lu, M., and Chopp, M. (2002). A test for detecting long-term sensorimotor dysfunction in the mouse after focal cerebral ischemia. J. Neurosci. Methods *117*, 207-214.

Zhang, R., Liu, Y., Yan, K., Chen, L., Chen, X.R., Li, P., Chen, F.F., and Jiang, X.D. (2013). Anti-inflammatory and immunomodulatory

mechanisms of mesenchymal stem cell transplantation in experimental traumatic brain injury. J. Neuroinflammation *10*, 106.

Zhao, X., Zhang, Y., Strong, R., Zhang, J., Grotta, J.C., and Aronowski, J. (2007). Distinct patterns of intracerebral hemorrhage-induced alterations in NF-kappaB subunit, iNOS, and COX-2 expression. J. Neurochem. *101*, 652-663.